Iranian Journal of Medical Physics

ijmp.mums.ac.ir

Evaluation of Dose Distribution in Lung Tumor Radiotherapy with Boron Neutron Capture Therapy

Mansour Zabihzadeh[1, 2, 3], Farnaz Rahimli[1 *], Mohammad Ali Behrooz[1], Amir Danyaei[1], Hodjatolah Shabazian[2]

1. Department of Medical Physics, Faculty of Medicine, Ahvaz Jundishapur University of Medical Sciences, Ahvaz, Iran
2. Department of Clinical Oncology, Faculty of Medicine, Golestan Hospital, Ahvaz Jundishapur University of Medical Sciences, Ahvaz, Iran
3. Cancer, Environmental and Petroleum Pollutants Research Center, Ahvaz Jundishapur University of Medical Sciences, Ahvaz, Iran

ARTICLE INFO

Article type:
Original Paper

Article history:
Received: Jun 13, 2019
Accepted: Dec 22, 2019

Keywords:
Boron neutron capture therapy (BNCT)
Organs at risk (OARs)
Lung cancer
Monte Carlo Simulation

ABSTRACT

Introduction: It is well known that neutrons are more effective treatments than photons to treat hypoxic tumors due to the interaction with the nucleus and the production of heavy particles. This study aimed to evaluate the suitability of Boron neutron capture therapy (BNCT) for the treatment of lung cancer. To this end, neutron dose distributions were calculated in lung tumor volume and peripheral organs at risk (OARs).

Material and Methods: Dose distribution to treat lung cancer was calculated by MCNPX code. An elliptical tumor with a volume of 27cm^3 was centered in the left lung of the ORNL phantom and was irradiated with neutron spectrums of Massachusetts Institute of Technology (MIT) and CNEA-MEC. The tumor was loaded with different concentrations of Boron 0, 10, 30, and 60 ppm to evaluate the delivered dose to OARs.

Results: Neutron absorbed dose rates in the tumor were 2.2×10^{-3}, 2.6×10^{-3}, 3.4×10^{-3}, and 4.7×10^{-3} Gy/s for boron concentrations of 0, 10, 30, and 60 ppm, respectively for MIT. Moreover, similar results for CNEA-MEC were 1.2×10^{-3}, 1.6×10^{-3}, 2.5×10^{-3}, and 3.7×10^{-3} Gy/s. The heart absorbed the maximum neutron dose rate of 1.7×10^{-4} and 1.6×10^{-4} Gy/s in MIT and CNEA, respectively. For all energy bins of spectrums, the neutrons flux is decreased as it penetrates the lung.

Conclusion: An increase in boron concentrations in tumors increases the absorbed doses while deteriorates dose uniformity. The results show that the MIT source is well suited to treat deep lung tumors while maintaining the OARs' dose within the threshold dose.

► *Please cite this article as:*
Zabihzadeh M, Rahimli F, Behrooz MA, Danyaei A, Shabazian H. Evaluation of Dose Distribution in Lung Tumor Radiotherapy with Boron Neutron Capture Therapy . Iran J Med Phys 2021; 18: 63-69. 10.22038/ijmp.2019.40980.1586.

Introduction

Lung cancer (both small cell and non-small cell) is the second most common cancer in both males and females. According to the American Cancer Society, the rate of lung cancer in the United States was 228,150 in 2019, and about 142,670 deaths resulted from this cancer [1]. The factors affecting the treatment of lung cancer include its location, stage, and the individual's overall health. Although the most commonly used methods for the treatment of lung cancer are surgery and radiation, chemotherapy could be used for small cell lung cancer. To improve the radiation treatment, it is crucial to deliver the maximum dose to cancerous tissues while minimizing the dose (fewer than the threshold) to normal tissues [2,3]. In general, radiotherapy utilizes photon and electron beams. The interaction of photon and electron beams with tissues caused cellular damage and cell destruction by the production of free radicals. The presence of oxygen fixes the DNA damages produced by free radicals [4], whereas the treatment efficacy (tumor dose to marginal normal tissue dose ratio) for photon and electron beams reduced for *hypoxygenated tumors. Moreover,* the therapy side effects would be significant due to the higher oxygen level around healthy tissue [5,6]. The collision of neutrons with tissues led to interaction with atomic nuclei and the creation of heavy fission fragments [7]. Therefore, it can overcome the limitation that is imposed by hypoxygenated tumors as a crucial parameter in radiotherapy by photon or/and electron beams [8]. Furthermore, fission fragments in neutron collision have high linear energy transfer (LET) which has the potential to impose a localized treatment [9,10]. In Boron neutron capture therapy (BNCT), modified neutron beams are used in the treatment of a target tissue filled with appropriate concentrations of boron components [11]. The BNCT technique includes two steps, namely filling the tumor with the correct amount of ^{10}B concentration (boron has a high cross-section with thermal neutrons) and the use of proper neutron spectra (contain thermal and epithermal neutron beams) [12-14]. The possible neutron reactions are outlined as below:

*Corresponding Author: Tel: (+98) 9163234428; Fax: (+98) 613-3332066; E-mail: farnazrahimli@gmail.com

$$^{1}n_{thermal} + {}^{10}B \rightarrow {}^{11}B^{*} \rightarrow {}^{7}\text{Li}\ (0.84\ \text{MeV}) + \alpha\ (1.47\ \text{MeV}) + \gamma\ (0.48\ \text{MeV}) \quad (94\%) \quad (1)$$

$$^{1}n_{thermal} + {}^{10}B \rightarrow {}^{11}B^{*} \rightarrow {}^{7}\text{Li}\ (1.01\text{MeV}) + \alpha\ (1.77\ \text{MeV}) \quad (6\%) \quad (2)$$

In the process of boron neutron capture in a target tissue, ^{10}B converted to ^{11}B and high energy recursive alpha particles and ^{10}Li ion are produced by ^{10}B(n,α)^{7}Li. These particles deposited their energy in the range of 4-10 μm (α particle~150 KeV/μm^{-1}, Li ion~175 KeV/μm^{-1}) that is comparable in size to cell dimension. Consequently, it can result in destroying tumor tissue with minimal damages to the normal tissues [13-16]. Another great advantage of the BNCT method is a high tendency of metastases cells in boron uptake, compared to healthy cells that cause boron accumulation in cancerous tissue that makes it possible to increase the treatment efficiency [9, 16].

According to other studies, it is not convenient to gain a desirable treatment efficiency by electron and photon beams in hypoxic lung tumors that are surrounded by the high amount of oxygen in peripheral healthy lung tissue [7]. In the cases that tumor tissue is within the lung, a fetal dose delivery to the target tissue is unavoidable [17]. Historically, the BNCT was used in clinical treatment to present a treatment plan on glioblastoma patients at Massachusetts Institute of Technology (MIT) and Brookhaven National Laboratory in the USA [18]. In this study, thermal neutrons irradiated as a primary beam to patients; however, the treatment efficacy was not favorable since the boron concentration in tumor to normal tissue ratio was low [19]. Due to the advancement in the drug delivery techniques, a new boron component called boronophenylalanine was administered that improved the cellular uptake results [20]. In 1990, the epithermal neutron beams were designed to irradiate the glioblastoma tumor in Brookhaven National Laboratory [21]. The utilization of these beams to treat the skin melanoma resulted in no interesting outcome due to penetrating deep tissues [22]. Currently, numerous generations of neutron accelerators are developed, and many efforts have been done to optimize the shape and energy of neutron beams to improve the neutron flux for clinical applications [11, 13, 23]. In the last decades, various treatment planning technique was suggested to improve BNCT outcomes in other cancer treatment types, such as liver, pancreas, and prostate [6, 24,25].

Despite significant progress, there are several limitations. Drug delivery needs fundamental improvements, and as far as boron agents are concerned, it is of paramount importance to develop the best dosing paradigms. However, they have not been optimized yet. For instance, it is necessary to modify the dosimetry for BNCT according to the real-time information on the boron content of the residual tumor to be irradiated since this dosimetry is still imprecise [18, 26]. However, research on BNCT and its radiotherapy parameters should be continued which needs more development in accelerator and improvement in clinical boron components [27]. Most previous investigations aimed to modify neutron sources and estimated organ doses for the treatment of high-grade gliomas and locally advanced cancers of the head and neck region as well as melanomas [18, 28]. According to the literature, there is little data for organ doses in BNCT of lung cancer that shows resistance in photon radiation treatment. Furthermore, lateral electronic *disequilibrium* in the *lung* is an obstacle to reach an accurate dose. Even with the most elaborate techniques, the accuracy better than 10% can rarely be achieved due to the limitations and complications for neutron measurement [29,30]. The Monte Carlo (MC) approach has high capabilities in calculating essential medical dosimetric quantities and has been implemented in pioneer MC based treatment planning system (TPS) to calculate optimized treatment plans.

In this study, two modified neutron beams with the Monte Carlo N-Particle Transport (MCNPX) code were used to evaluate the effect of neutron particles energy concerning the depth of penetration. The primary and secondary neutron fluxes were compared for their respective spectra. Furthermore, the dose distributions of the neutron beam in lung tumor volume and peripheral organs at risk (OARs) were calculated with different boron concentrations.

Materials and Methods

Phantom and Boron distribution

The MCNPX (version 2.6.0) code was utilized to calculate the dose distribution using BNCT for the treatment of lung cancer [31]. The anatomical simulation was performed using Oak Ridge National Laboratory (ORNL) phantom which is a mathematical human phantom [32]. The phantom included three tissue materials of the soft tissue, bone, and lung. An elliptical tumor with a volume of 27cm^3 was specified to a tumor. The tumor (P=7.1 gr/cm^3 [33]) was loaded separately with different ^{10}B concentrations (0, 10, 30, and 60 ppm), which is located at the center of the left lung. Mass density and composition (fraction by weight) of different tissues were adopted from report No. 44 of the International Commission on Radiation Units and Measurements (ICRU). The total density for each simulated model was calculated by weighting the share of each element of tumor tissue and using Boron concentration [34]. The positioning of the tumor in the left lung is challenging due to the proximity of heart tissue relative to the field of irradiation. The distribution of ^{10}B in tumor tissue was assumed to be uninformed. A rectangular field of the neutron was positioned at 10 cm surface source distance (SSD) to irradiate the target tissue.

Neutron spectra

A planar neutron field with dimensions of 3×3 cm^2 was modeled to cover the target tissue completely. The SSD was set at 10 cm to irradiate the tumor volume entirely in anterior-posterior (AP) directions (Figure 1). The irradiated spectrum was a parallel multi-energy beam sampled with the uniformly spatial distribution of neutrons.

In total, two neutron spectra were applied in the simulations as primary radiation to tumor tissue. Every spectrum was simulated separately in different files for various ^{10}B concentrations which contain 8 simulated files. The first spectrum was the recommended spectrum of Massachusetts Institute of Technology (MIT-SPECT) which optimized previously for clinical application and sampled with 10 KeV energy bin [35]. The second spectrum was the accelerator neutron source designed in Argentina named CNEA-MEC [36]. Both spectrums were optimized in beam shape and energy for medical applications and include the highest intensity in the range of epithermal neutron energy that is appropriate to treat deep-seated tumors. The primary spectra are shown in Figure 2.

Beams Validity

To validate the neutron beams, the present depth dose (PDD) curves in a water phantom were calculated for simulated MIT and CNEA beams and compared with published data by Riley et al. (2008). The details of source spectra and water phantom to mimic the neutron transport were defied based on the reported data by Riley et al. (2008). The calculated data for the PDD curves were in agreement with the results of the data reported by Riley et al. (2008). Moreover, they validated our defined characteristics of neutron sources (MIT and CNEA beams) to estimate the dose absorbed by lung tumor loaded with different concentrations of boron and the dose received by OARs. Each simulation was run separately for 10^7 neutron history to minimize the calculations errors.

Dose Calculation

In the BNCT method, the absorbed dose includes neutron dose (D_n) and gamma particles (D_γ). The absorbed dose delivered to the tumor, healthy lung, and other OARs consists of thermal, epithermal, fast neutrons, and gamma doses. The attenuated neutron and gamma fluxes were calculated by F4 tally. The corresponding doses to lung tumors and OARs, such as peripheral health lung tissue, heart, spinal cord, and right lung were determined by fluence to dose conversion factors using DE and DF cards.

$$H_t = W_n \times D_n + W_\gamma \times D_\gamma \quad (3)$$

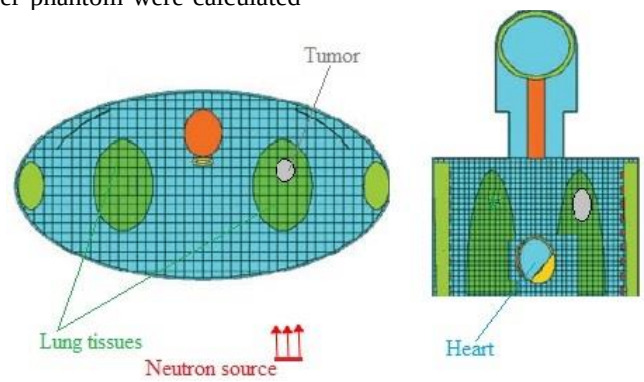

Figure 1. Cross-sectional views of the phantom. Lung tumor was located at the center of the left lung and the neutron source was positioned at SSD=10 cm

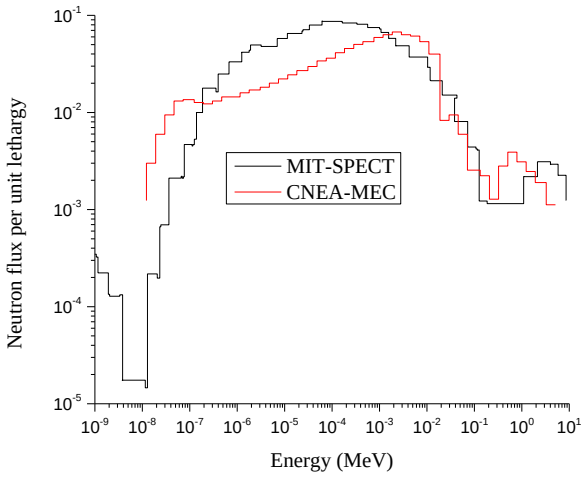

Figure 2. Relative neutron flux per unit lethargy as a function of energy for the MIT-SPECT and CNEA-MEC beams

Where H_t is the equivalent dose, D_n (Gy) signifies the neutron absorbed dose, D_γ (Gy) presents the alpha absorbed dose, and W_n, as well as $W\gamma$, are weighting factors for neutron and gamma beams, respectively. According to the ICRP 2007 report, the radiation weighting factor (W_n) depends on neutron energy. To simplify the calculations, the average value was selected for W_n. Therefore, W_γ is equal to 1, and W_n is considered to be 10 in calculations [37]. The neutron and photon doses were calculated by F6 Tally, and the neutron and gamma fluxes were quantified by F4 tally. All simulations were run for 4 $\times 10^7$ neutron history.

Results

The PDD curves were plotted (Figure 3) and the maximum depth (d_{max}) was compared to measured data reported by Riley et al. (2008). The d_{max} reported by Riley et al. (2008) for MIT beam was equal to 2.5 cm which is in agreement with our result [11]. Similarly, the d_{max} for CNEA beam was nearly 2.5 cm which agrees with our calculated d_{max}. In comparison, the PDD results of a designed neutron beam with an average of epithermal energy radiation in Snyder phantom possess the same d_{max} as in our study [38].

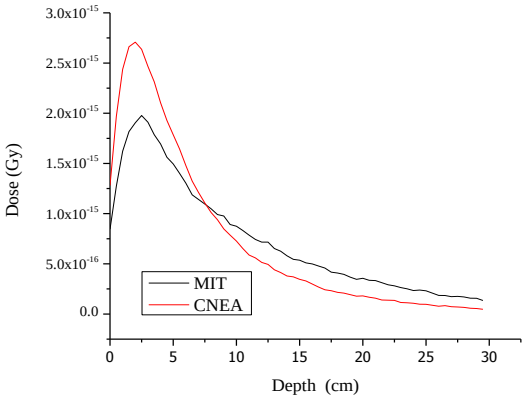

Figure 3. The PDD curves calculated for both neutron sources by the MCNPX code

The primary and attenuated spectra in the target tissue, healthy left lung, and right lung are presented in Figures 4a and 4b for MIT-SPECT and CNEA spectrum, respectively. The results of the MIT beam illustrate a dramatic decrease in neutron flux followed to penetrate lung tissue. Neutron flux declined in all energy bins of irradiated MIT spectrum. As shown in Figure 4a, the maximum fall-off occurred in the range of epithermal energy bins. Furthermore, the decreased neutron flux through the opposite lung (right lung) can be justified due to the spatial distribution of neutron particles. The result of the attenuated CNEA beam was similar to the MIT spectrum and showed a considerable reduction in epithermal neutrons.

Dose Calculation

In this calculation, the absorbed dose rate in tumor volume was equal to 1.17, 1.40, 1.86, and 2.55 Gy/min in MIT beam, and it was equal to 0.66, 0.89, 1.33, and 1.99 Gy/min in CNEA beam for boron concentration of 0, 10, 30, and 60 ppm, respectively. The absorbed dose in the lung tumor was increased with the enhancement of boron concentration. The equivalent dose in tumor and OARs tissues were calculated for clinical boron concentration of 30 ppm. The result of the calculations is reported in Table 1. The neutron flux was considered to be 10^{11} n/Cm^2.S, and the treatment time to deliver the lethal dose to the lung tissue was 27 and 37.2 min for MIT-SPECT and CNEA beams, respectively.

Boron Concentration Sensitivity

Based on the results, the neutron dose had no increase at the same rate for the two spectra as the boron concentration increased. As shown in Figure 5, when the boron concentration in lung tumor volume increases by 3 times (from 10 to 30 ppm), the neutron dose increase by 1.3 and 1.5 fold for MIT and CNEA beams, respectively.

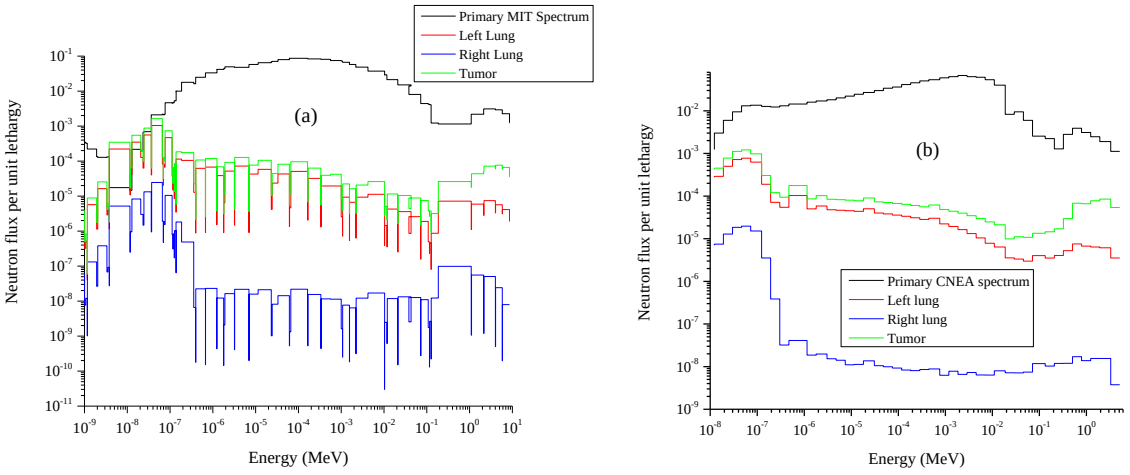

Figure 4. Primary and attenuated neutron flux in tumor and OARs for **a)** the MIT-SPECT beam and **b)** the CNEA-MEC beam

Table 1. The equivalent dose calculated for the MIT-SPECT and the CNEA-MEC beams for 30 ppm boron concentration

Organ	Equivalent Dose (Sv)	
	MIT-SPECT	CNEA-MEC
Tumor (left lung)	56.00	56.00
Marginal (health part) left lung tissue	4.31	4.81
Right lung	0.16	1.99
Heart	5.98	8.12
Spinal cord	0.43	0.57
Skin	0.39	0.54
Breast	1.49	2.00
Thyroid	0.1	0.20
Clavicle	0.20	0.34
Esophagus	0.45	0.58

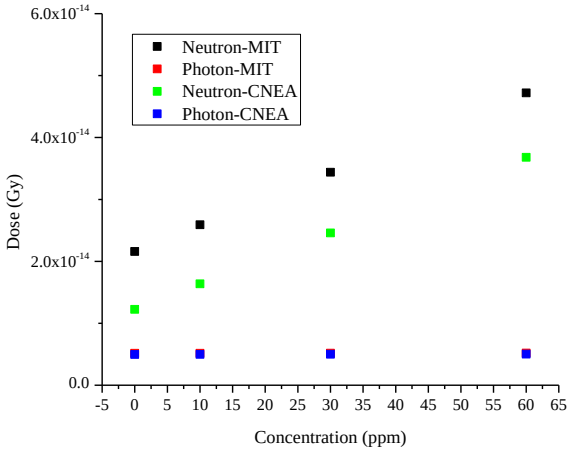

Figure 5. A comparison between neutron and photon absorbed doses in different boron concentrations in lung tumor volume for the MIT and CNEA spectra

Discussion

According to the results, the absorbed dose rate exceeded up to 37% in MIT and 50% in CNEA when the boron concentration of tumors increased from 30 ppm to 60 ppm. Therefore, the boron concentration and dose rate showed a direct correlation that can decrease the needed time to complete the treatment process and modify the dose homogeneity in the tumor area. The enhance dose factor in neutron absorbed dose was calculated for both neutron beams as the proportion of absorbed dose for 60 ppm boron concentrations. The results represent a reasonable increase of 2.2 and 3 times for MIT and CNEA beam, respectively. However, among the OARs, the heart tissue absorbed the maximum dose of 1.66 $\times 10^{-15}$ Gy (per neutron from source).

It can be seen from Table 1 that a neutron beam with more weighted fast neutron is not favorable in improving the dose to deep-seated tumor tissues unless dosimetry calculation and treatment design were optimized to reduce the dose to OAR's [7]. Among the OAR's, the heart received the maximum equivalent dose; however, it was still within the threshold dose (heart threshold dose for one session irradiation is 16 Gy) [39]. The standard tumor to normal tissue ratio factor in BNCT protocols is 2 or greater, and the ratio of absorbed dose in lung tumor to healthy left lung tissue was about 14 for 30 ppm. The ratio was approximately 5 for right lung tumors for 25 ppm boron concentration as reported by Krstic et al. (2014) [13]. This parameter was calculated from 2.3 to 3.2 for different irradiation fields and different simulated lung tumors in a study conducted by Farias et al. [9]. The delivered doses to OAR's were also greater than those reported in our data. This discrepancy is probably related to the differences in the techniques used by two studies.

Krstic et al. (2014) applied two opposite fields to irradiate the target tissue (anterior-posterior (AP) and posterior-anterior (PA) directions [13]. Moreover, Farias et al. (2014) used 3 and 5 multiple angular fields to irradiate the tumor tissue [9]; however, only the AP direction was simulated in the present study. In the same line, Farias et al. (2014) reported that the best tumor to normal tissue ratio was obtained with 3 fields (posterior, left anterior oblique, and right anterior oblique) [9]. The utilization of the multi-fields decreases the tumor to normal tissue ratio; nonetheless, it improves the uniformity of dose distributions in target volume with an increase in the minimum dose in the tumor area [9, 17].

The boron sensitivity outcomes in Figure 5 illustrate that by increasing the boron concentration, the number of boron atoms in target tissue increases which finally leads to the higher number of boron-neutron captures. Furthermore, according to Figure 5, the photon absorbed dose remains constant as the boron dose increased. Totally, three photon beams of 0.48, 0.58, and 2.2 MeV

are produced in nuclear reactions of boron-neutron, carbon-neutron, and hydrogen-neutron capture reactions, respectively. The main gamma dose is related to 2.2 MeV photons from the hydrogen-neutron capture reaction that could penetrate to the other OAR's and transfer its energy far from the produced location. Accordingly, they could cause no photon dose in the target volume. It is well known that boron has a high cross-section in thermal neutrons energy. Therefore, the primary epithermal neutrons lose energy by crossing the tissues and convert to thermal neutron in deep organs near the target tissue. The MIT spectrum has more epithermal neutrons; consequently, as mentioned above, the absorbed dose for this beam is higher than the CNEA beam.

Lung tumor movement due to respiration is a well-known complication and has been remained a major challenge in lung cancer radiotherapy. Gating radiotherapy based on lung tumor movement is a recommended technique to reach the accurate dose delivery. However, this dedicated technique has not been used in many departments yet due to some costly and technical limitations. Alternatively, the patients were recommended to hold their breath or breath as usual during CT scanning and radiation delivery. Furthermore, the feature of modeling the movement part in MC simulation is probably *not implemented* in MCNP codes.

Conclusion

The proposed simulated model in this study was successful in calculating the organ doses in the BNCT. A comparison in absorbed dose between tumor and normal lung tissue appears that BNCT results could be effective for cancer treatment. An increase in the boron concentration in lung tumors increases the absorbed dose while dose uniformity deteriorates. Our results show that the MIT neutron source is suitable to treat deep-seated lung tumors since OARs' dose could be limited within the threshold dose.

Acknowledgment

This study was extracted from an MSc thesis by Farnaz Rahimli, and funded by the Research Deputy Affairs of Ahvaz Jundishapur University of Medical Sciences, Ahvaz, Iran (Grant No. U-96101).

References

1. American Cancer Society. Key Statistics for Lung Cancer. 2019. availible from: https://www.cancer.org/cancer/non-small-cell-lung-cancer/about/key-statistics.html.
2. Bortolussi S, Altieri S. Thermal neutron irradiation field design for boron neutron capture therapy of human explanted liver. Med phys. 2007; 34(12):4700-5.
3. Khan FM, Gibbons JP. Khan's the physics of radiation therapy: Lippincott Williams & Wilkins; 2014.
4. Grimes DR, Partridge M. A mechanistic investigation of the oxygen fixation hypothesis and oxygen enhancement ratio. Biomed Phys Eng Express. 2015; 1(4):045209.
5. Hall EJ, Giaccia AJ. Radiobiology for the Radiologist: Lippincott Williams & Wilkins; 2006.
6. Mirzaei D, Miri-Hakimabad H, Rafat-Motavalli L. Depth dose evaluation for prostate cancer treatment using boron neutron capture therapy. J Radio Nucl Chem. 2014; 302(3):1095-101.
7. Yu H, Tang X, Shu D, Liu Y, Geng C, Gong C, et al. Influence of Neutron Sources and 10B Concentration on Boron Neutron Capture Therapy for Shallow and Deeper Non-small Cell Lung Cancer. Health Phys. 2017; 112(3):258-65.
8. Capoulat M, Kreiner A. A 13 C (d, n)-based epithermal neutron source for Boron Neutron Capture Therapy. Physica Medica. 2017; 33:106-13.
9. Farías RO, Bortolussi S, Menéndez PR, González SJ. Exploring Boron Neutron Capture Therapy for non-small cell lung cancer. Physica Medica. 2014; 30(8):888-97.
10. Zolfaghari M, Sedaghatizadeh M. Design and simulation of photoneutron source by MCNPX Monte Carlo code for boron neutron capture therapy. IJMP. 2015; 12(2):129-36.
11. Riley K, Binns P, Harling O, Albritton J, Kiger W, Rezaei A, et al. An international dosimetry exchange for BNCT part II: Computational dosimetry normalizations. Med phys. 2008; 35(12):5419-25.
12. Azahra M, Kamili A, Boukhal H. Monte Carlo calculation for the development of a BNCT neutron source (1ev‑10keV) using MCNP code. Cancer/Radiotherapie. 2008; 12(5):360-4.
13. Krstic D, Markovic V, Jovanovic Z, Milenkovic B, Nikezic D, Atanackovic J. Monte Carlo calculations of lung dose in ORNL phantom for boron neutron capture therapy. RPD. 2014; 161(1-4):269-73.
14. Rahmani F, Shahriari M. Beam shaping assembly optimization of Linac based BNCT and in-phantom depth dose distribution analysis of brain tumors for verification of a beam model. Annal Nucl Ener. 2011; 38(2):404-9.
15. Moss RL. Critical review, with an optimistic outlook, on Boron Neutron Capture Therapy (BNCT). Applied Radiation and Isotopes. 2014; 88:2-11.
16. Sweet W, Soloway A, Brownell G. Boron-slow neutron capture therapy of gliomas. Acta Radiologica: Therapy, Physics, Biology. 1963; 1(2):114-21.
17. Suzuki M, Suzuki O, Sakurai Y, Tanaka H, Kondo N, Kinashi Y, et al. Reirradiation for locally recurrent lung cancer in the chest wall with boron neutron capture therapy (BNCT). International Cancer Conference Journal; 2012: 1(4): 235-238.
18. Barth RF, Vicente MG, Harling OK, Kiger WS, Riley KJ, Binns PJ, et al. Current status of boron neutron capture therapy of high grade gliomas and recurrent head and neck cancer. Radiat Oncol. 2012; 7:146.
19. Farr LE, Sweet WH, Robertson JS, Foster CG, Locksley HB, Sutherland DL, et al. Neutron capture therapy with boron in the treatment of glioblastoma multiforme. Am J Roentgenol Radium Ther Nucl Med. 1954; 71(2):279-93.

20. Hatanaka H, Nakagawa Y. Clinical results of long-surviving brain tumor patients who underwent boron neutron capture therapy. IJROBP. 1994; 28(5):1061-6.
21. Chanana AD, Capala J, Chadha M, Coderre JA, Diaz AZ, Elowitz EH, et al. Boron neutron capture therapy for glioblastoma multiforme: interim results from the phase I/II dose-escalation studies. Neurosurgery. 1999; 44(6):1182-93.
22. Busse PM, Harling OK, Palmer MR, Kiger W, Kaplan J, Kaplan I, et al. A critical examination of the results from the Harvard-MIT NCT program phase I clinical trial of neutron capture therapy for intracranial disease. Journal of Neuro-oncology. 2003; 62(1):111-21.
23. Matsumoto T. Monte Carlo simulation of depth‐dose distribution in several organic models for boron neutron capture therapy. Nucl InstrumMethods Phys. Res A. 2007; 580(1):552-7.
24. Koivunoro H, Bleuel D, Nastasi U, Lou T, Reijonen J, Leung K. BNCT dose distribution in liver with epithermal D‐D and D‐T fusion-based neutron beams. Applied Radiation and Isotopes. 2004; 61(5):853-9.
25. Yanagie H, Sakurai Y, Ogura K, Kobayashi T, Furuya Y, Sugiyama H, et al. Evaluation of neutron dosimetry on pancreatic cancer phantom model for application of intraoperative boron neutron-capture therapy. Biomedicine & Pharmacotherapy. 2007; 61(8):505-14.
26. Gupta N, Gahbauer RA, Blue TE, Albertson B. Common challenges and problems in clinical trials of boron neutron capture therapy of brain tumors. J Neurooncol. 2003; 62(1-2):197-210.
27. Zonta A, Prati U, Roveda L, Ferrari C, Zonta S, Clerici A, et al. Clinical lessons from the first applications of BNCT on unresectable liver metastases. 2006; 41. J. Phys.: Conf. Ser. 2006; 41: 484.
28. Moss RL. Critical review, with an optimistic outlook, on Boron Neutron Capture Therapy (BNCT). Appl Radiat Isot. 2014; 88:2-11.
29. AAPM. Neutron Measurements Around High Energy X-ray Radiotherapy Machines. AAPM American Association of Physicists in Medicine. 1986;19.
30. Naseri A, Mesbahi A. A review on photoneutrons characteristics in radiation therapy with high-energy photon beams. Rep Pract Oncol Radiother. 2010; 15(5):138-44.
31. Pelowitz DB. MCNPXTM user’s manual. Los Alamos National Laboratory, Los Alamos. 2005.
32. Cristy M, Eckerman K. Specific absorbed fractions of energy at various ages from internal photon sources. VI. Newborn. ORNL/TM-8381. 1987.
33. Suryanto A, Herlambang K, Rachmatullah P. Comparison of tumor density by CT scan based on histologic type in lung cancer patients. Acta Med Indones. 2005; 37(4):195-8.
34. ICRU. ICRU Report No. 44, Tissue substitutes in radiation dosimetry and measurement; Bethesda: ICRU; 1989.
35. Kiger III W, Sakamoto S, Harling O. Neutronic design of a fission converter-based epithermal neutron beam for neutron capture therapy. Nuclear science and engineering. 1999;131(1):1-22.
36. Capoulat M, Minsky D, Kreiner A. Computational assessment of deep-seated tumor treatment capability of the 9Be (d, n) 10B reaction for accelerator-based Boron Neutron Capture Therapy (AB-BNCT). Physica Medica. 2014; 30(2):133-46.
37. ICRP. The 2007 Recommendations of the International Commission on Radiological Protection. ICRP publication 103. Ann ICRP. 2007;37(2-4):1-332.
38. Rasouli FS, Masoudi SF. Simulation of the BNCT of brain tumors using MCNP code: beam designing and dose evaluation. IJMP. 2012; 9(3):183-92.
39. Benedict SH, Yenice KM, Followill D, Galvin JM, Hinson W, Kavanagh B, et al. Stereotactic body radiation therapy: the report of AAPM Task Group 101. Med phys. 2010; 37(8):4078-101.